THE PIERRE AUGER OBSERVATORY FOR UHE COSMIC RAYS

G. NAVARRA for the Pierre Auger Collaboration
Department of General Physics and INFN, via P. Giuria,1
10125, Torino, Italy

The Southern site of the Pierre Auger Observatory is at about 50% of its realization, and the commissioned part of the array is taking data. The aim of the project is the study of cosmic radiation at the highest energies ($E_0 > 10^{18}$ eV), which is relevant for astrophysics and fundamental physics reasons. The experiment is based on the hybrid approach: combined surface and atmospheric fluorescence detection arrays. We present here the main properties of the detectors and the performances based on first experimental data.

1 Introduction

The understanding of the sources and of the propagation of the highest energy cosmic rays represents one of the most challenging problems in high energy physics and astrophysics. The theme is indeed dense of theoretical implications (both concerning the extreme astrophysical phenomena and fundamental physics problems) and stimulating experimental requirements. We remind that at such energies the measurements have to be based on the Extensive Air Shower technique, i.e. on the detection of the secondaries produced in the atmosphere by the primary particle. The event rate we have to face, at about 10^{20} eV, is $1/(100\ \mathrm{km^2 y})$, which determines the scale of the arrays and the duration of the data taking. Moreover we are very far from the energy and kinematics region at which we have direct accelerator data on the hadronic interactions cross sections, we are affected by the atmospheric variability, and (operating at fixed atmospheric depth) we are particularly sensitive to the fluctuations in the air shower development. The present experimental situation is summarized in fig. 1, showing the AGASA and Hires spectra above $5{\cdot}10^{18}$ eV (for references see review[1]). The two experiments are based on the two mainly exploited techniques: detectors of the charged particles at the ground level, and of the fluorescence light produced by the charged particles in the atmosphere. The systematic difference between the two spectra corresponds to about 20% in absolute energy calibration.

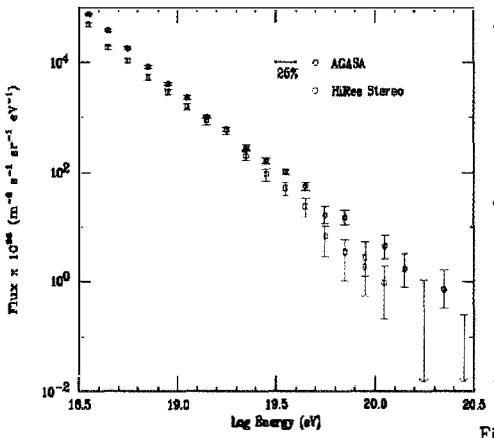

Figure 1: Primary spectra in the highest energy region as reported by AGASA and HiRes (stereo data)[2].

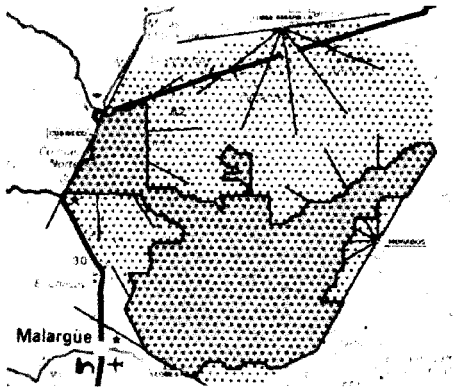

Figure 2: Plan of the Southern P. Auger Observatory (each point represent an SD tank) and status on March 2005 (SD: darker, FD: the two eastern eyes completed).

Such difference is large but not striking for such kind of measurements. More divergent are the results above 10^{20} eV, where against 11 events observed by AGASA, the HiRes spectrum seems abruptly broken. The presence of primaries above 10^{20} eV can however be considered established also by the fluorescence technique, as demonstrated by the event of about $3{\cdot}10^{20}$ eV reported by Fly's Eye in 1991. The spectral shape above 10^{20} eV is indeed very significant, since in such region the primary nuclei loose energy interacting with the universal blackbody radiation (for the case of photo-pion production by protons, the so called GZK effect). The primary spectrum is affected by such energy losses if the cosmic rays path (i.e. the distance of the sources) exceeds about 100 Mpc. Therefore, if no effect is observed, as in the case of the AGASA spectrum, we should conclude that the sources are located at distances d < 100 Mpc. The knowledge of extragalactic magnetic fields is rather poor, but we know that they have random components and do not exceed values of the order of nG. In such conditions the maximal angular deviation of a proton of 10^{20} eV, for a total path-length of 100 Mpc, is of the order of a few degrees, and therefore we should expect that the events accumulate around the directions of their sources. Such an effect could have been marginally observed by AGASA. Notice that we are treating such primaries as of extragalactic origin mainly due to the absence of large anisotropies (and insufficient containment by our Galaxy), but the transition from the galactic to the extragalactic contribution has still to be established. From the point of view of fundamental physics, we have to remark that if the described astrophysical scenario would be insufficient, we should look for other explanations, i.e. to the possibility that such events are due to different, new processes (we remind, among others, the proposed decays of super-symmetric particles in the galactic halo). We need therefore: a) an improved energy determination, not strictly dependent on the hadronic interaction model used for the interpretation; b) contemporaneous "surface" and "fluorescence" observation of the same events in order to fix the energy scale; c) improved statistics above the GZK energy in order to describe the spectrum in such region, and to search for potential "sources" (or at least anisotropies, that could reveal a relationship with the source distribution); d) an approach to the composition and evolution of the composition vs. primary energy (energy dependent effects depend on the primaries, as e.g. the interpretation of the "dip" observed by different experiments between 10^{18} and 10^{19} eV); again the dependence on the hadronic interaction models has to be disentangled.

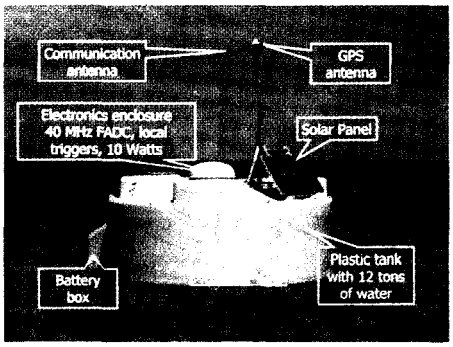

Figure 3: View of a tank: the main elements are shown.

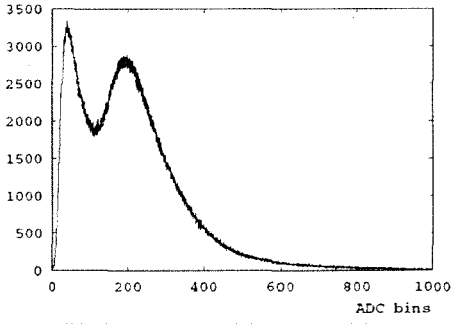

Figure 4: The "muon hump": basic measurement for the SD calibrations. The plot represents the distribution of the total three PMT output obtained triggering in threefold coincidence.

2 The Auger Project

The Auger Project [2,3] was therefore planned to fulfill such experimental requirements, by combining surface and fluorescence detectors operating in conjunction over extremely wide collecting areas. Two observatories, both in the Southern and in the Northern emispheres will be realized, to obtain the required full sky coverage. The Southern site, now under construction, is located in the proximity of Malargue (province of Mendoza, Argentina), in a flat region called Pampa Amarilla at 1400 m above sea level, atmospheric depth 875 g/cm^2, latitude -35.5^o.

2.1 The Surface Detector (SD)

The Surface array (see fig. 2) is based on 1600 water tank detectors (10 m^2 base, 1.2 m height, see fig. 3), spaced of 1500 m from each other, in a triangular grid, and covering an area of 3000 km^2. The power supply is provided by solar panels, through batteries (the total power comsumption is limited to 10 W); communications are realized through a radio network; the timing of the events is obtained by GPS with measured accuracy of about 8 ns. The Cherenkov light produced by ultrarelativistic particles (and diffused by a tyvek liner inside the tank) is detected by means of three 9" diameter photomultipliers. The anode and amplified ($\times$ 32) dynode signals of the PMTs are sampled at a rate of 40 MHz, producing continuous records (two 10 bits FADCs). The overall dynamical range is of 15 bits (starting from 1/50 of a muon, with linearity better than 5%). A hierarchical trigger sequence selects the occurring of events from the local station (in "threshold" and "time over threshold" modes, the latter mainly efficient for selecting events at large core distances), to the central DAQ system (selecting at least three fired stations in a compact configuration). For hadronic events, 100% efficiency is reached at the primary energy of about $3{\cdot}10^{18}$ eV. Continuous calibrations and monitoring procedures, that are obviously of main importance for a detector which is spread over thousands of km^2 and has to run stably for many years, are guaranteed by the muon flux (about 3 kHz). An example of the "hump" due to the omnidirectional muon flux in a tank is shown in fig. 4. The peak can be selected with high precision and followed during time (which is quite important, manly because of the changing temperature of the whole ensemble, ranging up to about 30°C every day). The "hump" is converted to the signal due to a single vertical muon crossing the tank in its center (VEM, about 100 p.e./PMT)), which is the unit used for LDF and energy reconstruction.

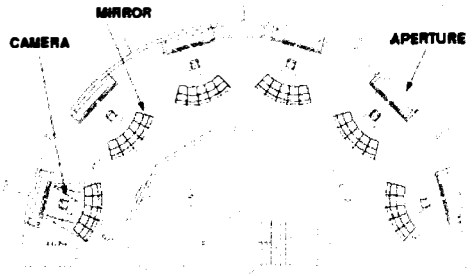

Figure 5: Scheme of a fluorescence detector eye.

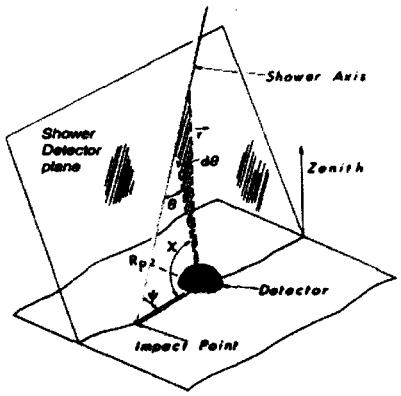

Figure 6: EAS detection in fluorescence light.

2.2 The Fluorescence Detector (FD)

The FD is made by four eyes (see figs. 2 and 5) with six mirrors each covering a 30°(azimuth) x 28.6° (elevation) angular field of view per mirror, located at about 50 km from each other. The optical aperture is 3.8 m^2 (Schmidt optics, including at the edges a corrector ring to compensate for the spherical aberrations), and is closed by an optical filter, selecting the wavelength range $300 < \lambda < 400$ nm, i.e. the Nitrogen fluorescence region. Each mirror (A=11 m^2 is viewed by a matrix of 440 PMTs at focal distance of 1.7 m); the angular aperture of each PMT pixel is of 1.5°. The absolute pointing of each pixel is measured exploiting the signals of the through-going stars in its field of view: the average orientations of the Los Leones mirrors (which have the longest live time) are thus determined with precision at the level of 0.1°. The PMT outputs are read with 10 MHz sample (12 bits ADC, 15 bits dynamic range). The hierarchical trigger is based on adjustable thresholds on the individual channels, up to the selection of triggering patterns compatible with air shower traces. The energy threshold for nearby events is $E_t^{FD} \approx 10^{17}$ eV. The end-to-end calibration of the chain is obtained by means of monthly measurements performed with a "drum" with internal teflon surfaces illuminated by an UV-LED (the LED being monitored by a PMT, absolutely calibrated by a NIST photodiode: the resulting calibration constant is about 4.0 photons/ADC count, established and monitored at better than 10%). The relative calibrations are continuously followed by means of UV lamps, while a continuous monitoring is provided by the study of the fluctuations of the night-sky background. The atmospheric transparency is a main factor for the FD (light for distant events can travel more than 30 km in horizontal direction); it is therefore continuously monitored through different complementary techniques operating at the same time, such as cloud monitors, steerable lidar systems, a laser beam facility. Regular balloon flights provide continuous pressure and temperature profiles of the atmosphere.

A scheme showing the detection principle of the EAS fluorescence light is shown in fig. 6. The EAS core is seen as a track in the PMT matrix; the angle (θ) is determined through the times of flight between the different PMTs. The knowledge of the "impact point" from the SD array provides the complete definition of the geometry. Such "hybrid" events beside an improved geometry reconstruction, provide parallel SD and FD data and therefore the possibility of crossed inter-calibrations (most important for energy determinations and check of the absolute direction accuracies of the SD reconstruction). While the SD is active for 100% of the time, and therefore is the main tool for reaching the required statistics, the FD detectors can operate

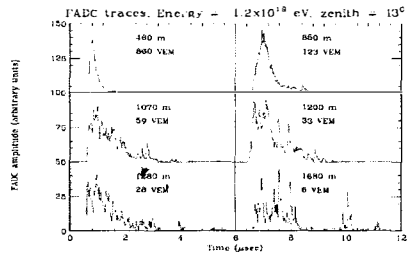

Figure 7: Typical shapes for a "vertical" shower event. Notice the wide temporal spreads, and the steep lateral distribution.

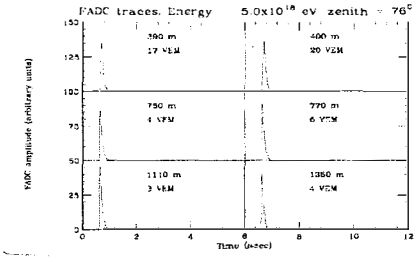

Figure 8: Typical shapes for an "inclined" shower event. The temporal widths are very narrow, and the lateral distribution is smooth: only muons are detected.

only in dark, clear New Moon nights, and therefore with a duty cycle of the order of 10%. The fluorescence detector data can provide an absolute energy calibration, since the number of photons at the aperture of the optical system can be converted, through the EAS geometry, to the number of charged particles (i.e. electrons) along the shower development (providing a "calorimetric" approach). The fundamental calibration factor is thus the fluorescence yield, i.e. the number of fluorescence photons produced per unit of path length. Such factor (about 4.8 photons/(electron×m)) is now known with an uncertainty of about 15% and represents a main source of systematic uncertainties for the energy determination.

3 The data

The status of the array is shown in fig. 2. We present here a few events showing the principles of the analysis and the quality of the information.

Concerning the SD, the structure of the detectors (i.e. a significant acceptance not only for vertical, but also for inclined particles) allows the shower detection over a very large range of zenith angles. In figs. 7 and 8 two typical events observed respectively at 13 and 76 degrees are shown. Their characteristics are quite different from the point of view of the temporal and lateral spreads, due to the dependence on the shower stage of development. The pulse shape brings information on the e.m. component and the muons, including their production heights. Very inclined events look always "old", since they are originated very far in the atmosphere. A "young" shower observed at a large zenith angle should be due to a deeply penetrating particle, a feature that makes Auger the most sensitive detector for a possible tau neutrino flux at primary energies around 10^{18} eV.

As an additional example, an hybrid-stereo event (i.e. an event observed both by the surface and the fluorescence detectors, from two of its eyes) is shown in fig. 9 concerning the SD, together with the reconstructed lateral distribution. As best estimator of the primary energy, the signal at 1000 m from the core is used. The core location as obtained from the fit to the SD densities is compared in fig. 10 to the one obtained from the FD data (i.e. the crossing of the two observation planes from the two eyes). The event as seen by one of the FD eyes is shown in fig. 11, together with the derived longitudinal profile (fig. 12). Such event combines the stereo and hybrid concepts. The statistical uncertainties in the reconstruction of hybrid events of 10^{19} eV are $\delta\theta \approx 0.3^o$ for the arrival direction, $\delta r \approx 20$ m for the core location, $\delta E_0/E_0 \approx 7\%$ for energy determination, $\delta X_{max} \approx 25$ g·cm^{-2} for the depth of shower maximum (the observable which is strictly related to the mass of the primary). In the event under consideration the SD and FD independent energy determinations are quite consistent, about (7-8)×10 ^{19} eV.

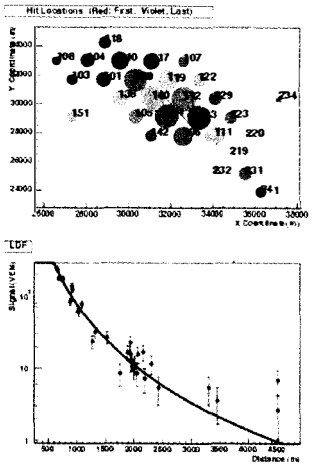

Figure 9: Example of an hybrid-stereo event as seen by the SD. The reconstructed LDF is also shown.

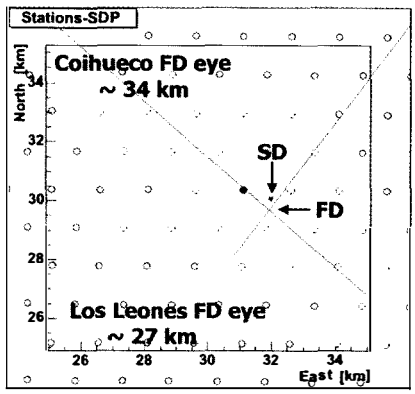

Figure 10: Identification of the impact of the shower axis on the ground as obtained by the intersecting shower planes identified by the two FD eyes, compared with the reconstructed core position from the fit to the SD densities.

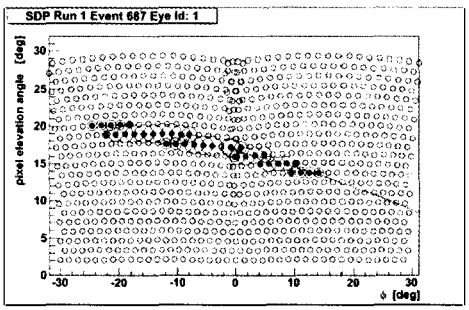

Figure 11: Track of the shower in the two mirrors of a FD eye.

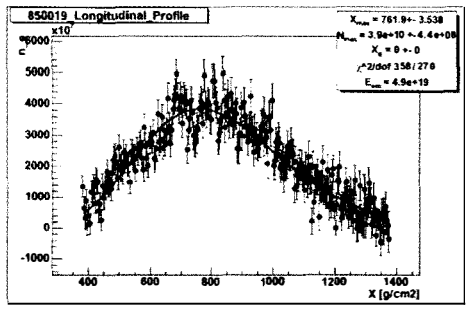

Figure 12: Longitudinal shower profile as obtained from the readings of fig. 11.

4 Conclusions

At present (May 1, 2005) 750 tanks of the SD are in operation, together with 2 full fluorescence eyes (Los Leones and Coihuecho, for a third one the infrastructure is completed and the installation is on the way). 120,000 SD events are available for analysis; 16,500 have tank multiplicity m$\geq$ 4 and primary energy $E_0 \geq 10^{18}$ eV. The event rate is about one per tank per day. The number of hybrid events, that we consider the "foundations" of the energy measurements, is 1750, of which 350 "golden" i.e. with both detectors fulfilling both triggering conditions (much less information is sufficient for the hybrid reconstruction technique). The data themselves show the quality of the information. The completion of the South site array is foreseen in 2006; first physical data will be released in the summer of 2005.

References

1. M.Nagano, A.A.Watson, *Rev. Mod. Phys.* **27**, 689 (2000).
2. J.W.Cronin, *Nucl. Phys.* B **138**, 465 (2005)
3. Auger Collaboration, *Nucl. Instrum. Methods* A **523**, 50 (2004).